Journal of Marine Systems 109–110 (2013) 138–148

Contents lists available at SciVerse ScienceDirect

Journal of Marine Systems

journal homepage: www.elsevier.com/locate/jmarsys

Phytoplankton carbon and chlorophyll distributions in the equatorial Pacific and Atlantic: A basin-scale comparative study

Xiujun Wang [a,b,*], Raghu Murtugudde [a], Eric Hackert [a], Emilio Marañón [c]

[a] Earth System Science Interdisciplinary Center, University of Maryland, College Park, MD 20740, USA
[b] College of Global Change and Earth System Science, Beijing Normal University, Haidian, Beijing 100875, China
[c] Departamento de Ecología y Biología Animal, Universidad de Vigo. 36200 Vigo, Spain

ARTICLE INFO

Article history:
Received 22 June 2011
Received in revised form 13 January 2012
Accepted 19 March 2012
Available online 31 March 2012

Keywords:
Phytoplankton carbon biomass
Chlorophyll
C:Chl ratio
Equatorial Pacific
Equatorial Atlantic

ABSTRACT

Satellite datasets show higher chlorophyll concentration in the surface water of the equatorial Atlantic relative to that of the equatorial Pacific. Is the phytoplankton biomass also higher in the Atlantic? To answer this question, a basin-scale ocean circulation-biogeochemistry model that has a phytoplankton dynamic model is utilized to compare the spatial and temporal variations of phytoplankton carbon biomass. We use field data collected in the equatorial Atlantic to derive a new set of biological parameters so that the model can reproduce the general features of the phytoplankton biomass and chlorophyll in this region. For instance, the model reproduces the observed deep chlorophyll *a* maximum (DCM) that is much deeper to the south (~100 m) of the equator than to the north (~70 m). The simulated surface chlorophyll also compares well with the satellite derived chlorophyll at basin scale for the equatorial Atlantic. Our comparative analyses demonstrate that for the upwelling region, the phytoplankton biomass in the surface water is considerably higher in the equatorial Pacific than in the equatorial Atlantic. However, for the entire euphotic zone, the integrated phytoplankton biomass is much higher in the equatorial Atlantic than in the Pacific. The difference in the surface water simply reflects larger phytoplankton carbon to chlorophyll ratios in the equatorial Pacific, due to strong iron limitation. The difference in the subsurface water is due to a pronounced deep biomass maximum (DBM) existing in the equatorial Atlantic, which is associated with higher nitrate in the lower euphotic zone. This modeling study emphasizes the importance of using variable C:Chl ratios to estimate carbon biomass at regional to global scales.

1. Introduction

The equatorial oceans play a large role in the global carbon cycle because of their vast expanse. However, there are limited studies of carbon biomass for the equatorial oceans due to the limitations in observational methodology. Phytoplankton carbon biomass is usually estimated from cell bio-volume and abundance through the microscopic measurement and flow cytometry (*e.g.*, Brown et al., 2003; Chavez et al., 1996; Ishizaka et al., 1997; Maranon et al., 2000), which is time-consuming and thus impractical to be employed routinely in field studies. As an alternative solution, phytoplankton biomass is often inferred from chlorophyll *a*, a pigment that is common to all planktonic autotrophs and can be easily measured, *e.g.*, using remote sensing techniques.

Over the past two decades, there has been a continuous record of satellite derived global distribution of chlorophyll, *i.e.*, the Sea-viewing Wide Field-of-view Sensor (SeaWiFS) chlorophyll (McClain et al., 2004). The SeaWiFS chlorophyll dataset has been used widely, *e.g.*, for the estimations of the global oceanic primary productivity (Behrenfeld and Falkowski, 1997; Behrenfeld et al., 2005; Carr et al., 2006; Westberry et al., 2008), and the validation of biogeochemical and ecosystem models (Doney et al., 2009; Faure et al., 2006; Lefevre et al., 2003; Wang et al., 2009a). However, these approaches rely on the knowledge of converting chlorophyll concentration to phytoplankton carbon biomass.

The relationship between phytoplankton carbon biomass and chlorophyll concentration is non-linear because of the complex influences of light, nutrients and temperature, and the different responses of various phytoplankton groups (Armstrong, 2006; Behrenfeld et al., 2002, 2005; Brown et al., 2003; Geider et al., 1996, 1997, 1998; Le Bouteiller et al., 2003; Wang et al., 2009a). For instance, the surface C:Chl ratio varies from <80 g:g in the upwelling region to >200 g:g in the oligotrophic region of the equatorial Pacific Ocean (Le Bouteiller et al., 2003). However, little has been done to evaluate the large-scale spatial and temporal variations in C:Chl ratio across basins, which hampers our ability to utilize the satellite-derived chlorophyll dataset. The SeaWiFS chlorophyll is higher in the equatorial Atlantic than in the equatorial Pacific (Fig. 1). One would

* Corresponding author at: 5825 University Research Ct, College Park, MD 20740, USA. Tel.: +1 301 405 1532; fax: +1 301 405 8468.
E-mail address: wwang@essic.umd.edu (X. Wang).

0924-7963/$ – see front matter © 2012 Elsevier B.V. All rights reserved.
doi:10.1016/j.jmarsys.2012.03.004

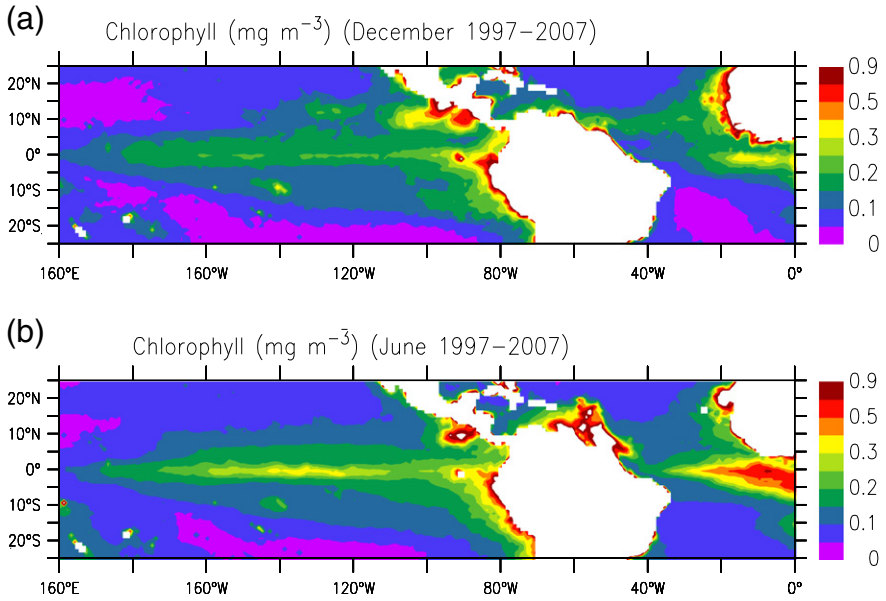

Fig. 1. Climatology (1997–2007) of SeaWiFS chlorophyll for (a) December and (b) June in the tropical Pacific and Atlantic.

ask: is phytoplankton carbon biomass also higher in the equatorial Atlantic than in the equatorial Pacific?

The equatorial Pacific is characterized by two distinct regions: the upwelling region in the central and eastern Pacific and the warm pool to the west (Le Borgne et al., 2002; Picaut et al., 2001) whereas the equatorial Atlantic is fairly narrow in its zonal extent and only referred to as an upwelling region (*e.g.*, Signorini et al., 1999 and Richard Barber, personal communication, 2010). A large number of observational and modeling studies have shown significantly zonal variability which is associated with interannual variability in many biogeochemical fields in the equatorial Pacific Ocean (Chavez et al., 2002; Feely et al., 2002; Le Borgne et al., 2002; Monger et al., 1997; Wang et al., 2005). However, studies have characterized profound seasonality in the physical and biogeochemical fields of the equatorial Atlantic (Busalacchi and Picaut, 1983; Christian and Murtugudde, 2003; Foltz and McPhaden, 2004; Grodsky et al., 2008). These contrasts would have implications for phytoplankton dynamics.

We have developed a dynamic model with varying C:Chl ratios as a function of four environmental variables, *i.e.*, irradiance, nitrate and iron concentrations and temperature (Wang et al., 2009a). The dynamic model, implemented into a basin-scale physical–biogeochemical model, reproduces well the general features of phytoplankton dynamics in the equatorial Pacific, including not only the zonal, meridional and vertical variations but also the interannual variability. In this study, we employ our basin scale model to compare the spatial and temporal variations in phytoplankton carbon biomass in the equatorial Pacific and Atlantic Oceans. Our study includes two major parts. We first use *in situ* data collected during the Atlantic Meridional Transect (AMT) Programme (http://web.pml.ac.uk/amt/) to calibrate and validate the phytoplankton dynamic model for the equatorial Atlantic. We then carry out detailed comparative analyses of phytoplankton carbon and chlorophyll between the equatorial Pacific and Atlantic, focusing on the upwelling regions for the period of 1990–2007.

2. Materials and methods

2.1. Model description

A fully coupled 3-dimensional physical–biogeochemical model has been developed for the equatorial Pacific and Atlantic Oceans. The ocean general circulation model (OGCM) is a reduced-gravity, primitive-equation, sigma-coordinate model that is coupled to an advective atmospheric mixed layer model (Gent and Cane, 1989; Murtugudde et al., 1996). The OGCM has 20 vertical layers with variable thicknesses. The upper-most layer, the mixed layer, is determined by surface turbulent kinetic energy generation, dynamic instability mixing, and convective mixing to remove static instabilities (Chen et al., 1994). The model is set up for a domain between 30°S and 30°N with zonal resolution of 1°, and variable meridional resolutions of 0.3–0.6° between 15°S and 15°N (1/3° at latitudes <10°), increasing to 2° at the northern and southern boundaries. In the sponge layer (10° band) near the boundaries, temperature, salinity, and nitrate are gradually relaxed back toward climatology.

The model is forced by solar radiation, cloudiness, surface wind stress, and precipitation. Air temperature and humidity are computed by the atmospheric mixed layer model. The solar radiation, precipitation, and cloudiness are climatological monthly means. The surface wind stresses are interannual, 6-day means from the National Centers for Environmental Prediction (NCEP) reanalysis (Kalnay et al., 1996). Interannual wind stresses are used to calculate latent and sensible heat fluxes which are the most important surface forcings at interannual time-scales in the tropics. Initial conditions are taken from the outputs of a climatological run which has been spun up for 30 years with initial conditions from Levitus. We perform an interannual simulation starting from 1980, and use model outputs from the period of 1990–2007.

The biogeochemical model consists of ten components: seven biological pools and three nutrients (ammonium, nitrate, and dissolved iron). The biological pools include dissolved organic nitrogen, and two size classes each (large and small) of phytoplankton, zooplankton and detritus. Model structure, equations and biogeochemical parameters were given by Wang et al. (2008). All biological components are carried in terms of their nitrogen currency, and computed in a similar manner to physical variables for all the layers. We apply a constant Redfield carbon to nitrogen (C:N) ratio (6.625) to compute phytoplankton carbon biomass. Our approach of applying a constant C:N ratio may have implications for phytoplankton carbon estimations in nitrogen limited systems (Geider and La Roche, 2002). However, the uncertainties or potential errors would be small in the tropical oceans because a field study showed a relatively small range in the phytoplankton C:N uptake ratio along a meridional transect crossing mesotrophic and oligotrophic waters (Raimbault et al., 1999).

A dynamic model that computes the phytoplankton carbon to chlorophyll (C:Chl) ratio as a function of light (I), nutrients (NO_3, Fe)

and temperature (T) has been implemented in a basin-scale ocean circulation-biogeochemistry model and validated for the equatorial Pacific Ocean (Wang et al., 2009a). Briefly, the model computes C:Chl ratio (η) as:

$$\eta = \eta_0 - (\eta_0 - \eta_{MIN}) \frac{\ln I_0 - \ln I}{4.605}, \quad (1)$$

$$\eta_0 = \eta_{MAX} - k_P \mu_0^*, \quad (2)$$

$$\mu_0^* = \mu_0 e^{k_T T} \min\left(\frac{NO_3}{K_N + NO_3}, \frac{Fe}{K_{Fe} + Fe}\right), \quad (3)$$

where η_{MAX} is the maximum C:Chl ratio near the surface, and η_{MIN} the minimum C:Chl ratio at the bottom of the euphotic zone. The term I_0 is the layer-averaged photosynthetically available radiation (PAR) in the mixed layer, k_P the slope of C:Chl ratio vs. growth rate. The term μ_0 is the maximum growth rate at 0 °C, and k_T the temperature dependence coefficient for phytoplankton growth. K_N and K_{Fe} are the half saturation constants for nitrogen and iron limitations on phytoplankton growth, respectively.

2.2. Field data and model calibration for the equatorial Atlantic

In situ data of chlorophyll and carbon biomass were collected during the AMT1-3. Chlorophyll *a* concentration was determined with the fluorometric method and phytoplankton carbon biomass was estimated from measurements of cell abundance and biovolume obtained with the flow cytometry and optical microscopy (Maranon et al., 2000).

Similar to the approach of Wang et al. (2009a), we use the observed phytoplankton carbon and chlorophyll from the AMT3 (see transect in Supplement Fig. 1) to calibrate the dynamic model for the equatorial Atlantic. This approach leads to reduced values of some biological parameters for the equatorial Atlantic, relative to the equatorial Pacific (Table 1). For example, the maximum C:Chl ratios of small and large cells change from 200 to 120 g:g in the equatorial Pacific to 115 and 70 g:g in the equatorial Atlantic, respectively. The smaller values of the half saturation constants reflect adaptation of phytoplankton to oligotrophic conditions (Huete-Ortega et al., 2011).

Fig. 2 presents the observed and modeled vertical–meridional distributions of chlorophyll for September–October, 1996. The modeled chlorophyll concentration is approximately 0.2 mg m^{-3} near the surface between 15°S and 15°N, which agrees well with the observations. Both the simulation and observations clearly show a deep chlorophyll maximum (DCM), which shoals from approximately 120 m near 15°S to <75 m near 15°N. The chlorophyll concentration ranges from ~0.25 to >0.5 mg m^{-3} at the DCM depth, with significantly higher values to the north than to the south of the equator.

Table 1
Different values of biological parameters used for the tropical Pacific and Atlantic.

Parameter	Symbol	Unit	Small		Large	
			Pacific	Atlantic	Pacific	Atlantic
Half saturation constant for N limitation	K_N	nmol m^{-3}	0.2	0.1	0.6	0.2
Half saturation constant for iron limitation	K_{Fe}	nmol m^{-3}	14	12	150	100
Minimum C:Chl ratio	η_{MIN}	g:g	30	25	15	15
Maximum C:Chl ratio	η_{MAX}	g:g	200	115	120	70
Photoacclimation coefficient	k_P	(g:g) d^{-1}	95	50	70	40

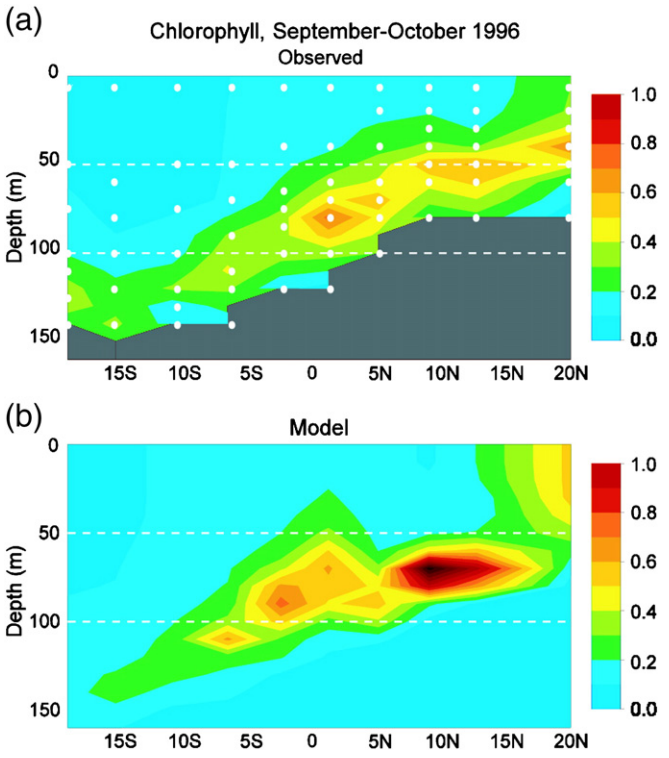

Fig. 2. Chlorophyll (mg m^{-3}) distribution along the AMT3 transect from (a) *in situ* measurement and (b) model simulation. Black area in (a) correspond to missing data.

The available observations suggest a deep biomass maximum (DBM) north of the equator, approximately coinciding with the DCM (Fig. 3). The observed carbon biomass exhibits a cross-equatorial extension that appears to shallow northward, showing surface phytoplankton carbon biomass of ~4–16 mg m^{-3} and DBM

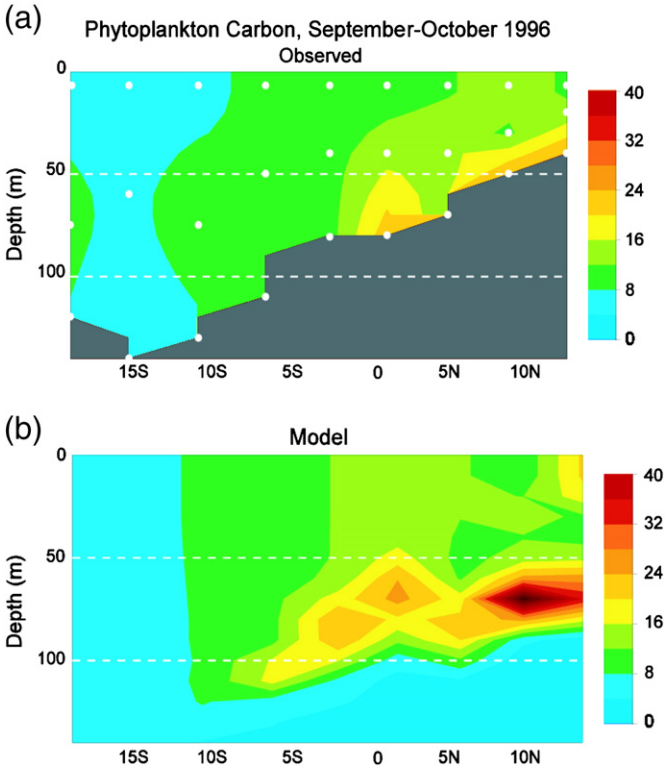

Fig. 3. Phytoplankton carbon biomass (mg C m^{-3}) along the AMT3 transect from (a) *in situ* measurement and (b) model simulation. Black area in (a) correspond to missing data.

phytoplankton biomass of ~24 mg m^{-3}. The model reproduces the general features of the observed carbon biomass, including meridional and vertical distributions. Both the simulation and observations indicate that DBM does not appear to the south of 10°S, which is distinct to DCM.

While the model simulation shows a general agreement with the observations, there are some differences. The model underestimates the chlorophyll concentration at the DCM between 10°S and 15°S, but overestimates it between 10°N and 15°N. These minor differences may be explained by the fact that field data is gathered at fine spatial and temporal resolutions that are not resolved by most models. For example, field measurements often represent some events occurring at much shorter time scales which can range from hours to days whereas our model is limited by the frequency of six-day wind forcing, and model simulations mostly represent mean conditions at much longer time scales (weeks to months).

3. Results

3.1. Model validation for the equatorial Atlantic

Our previous study showed that the basin scale model did a good job in reproducing sea surface temperature (Christian and Murtugudde, 2003). Here, we show model-data comparison of nitrate for the period of September–October, 1996 (Fig. 4). Nitrate concentration in the surface water is slightly higher in the model (0.5–1.5 mmol m^{-3}) than in the observations (<0.5 mmol m^{-3}). However, the model reproduces the main feature of the observed nitrate in the subsurface water, *i.e.*, shoaling of the nitracline from the south (~150 m) to the north (~50 m).

We also compare modeled phytoplankton carbon with the observations during the AMT2 (see Maranon et al., 2000). Fig. 5 illustrates that the model does a reasonable job in reproducing the spatial distributions of phytoplankton carbon. For example, both the model and observations show that phytoplankton carbon concentration in the

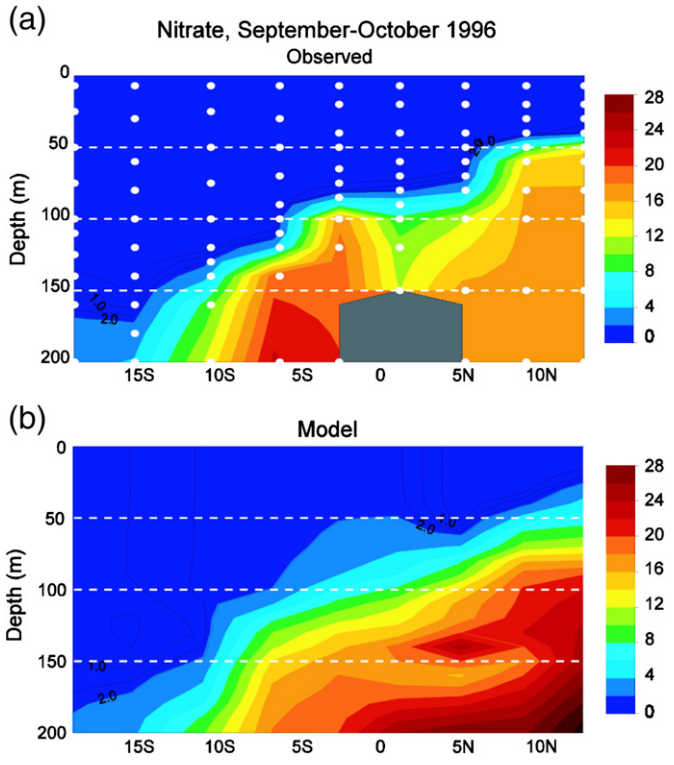

Fig. 4. Nitrate (mmol m^{-3}) distribution along the AMT3 transect from (a) *in situ* measurement and (b) model simulation. Black area in (a) correspond to missing data.

area of 8°N–12°N is approximately twice of that in the area of 10°S–15°S.

We then validate model simulation for the Atlantic basin by comparing the modeled surface chlorophyll with the SeaWiFS dataset. Fig. 6 presents a comparison of the climatology for the period of 1997–2007. The simulated chlorophyll concentrations in the surface water range from <0.1 mg m^{-3} south of the equator to >0.2 mg m^{-3} in the eastern upwelling region, which is consistent with the SeaWiFS derived chlorophyll. The modeled chlorophyll is generally smoother, possibly due to smoothing of the NCEP winds (Jiang et al., 2008). On the other hand, the SeaWiFS chlorophyll datasets may also have biases in the equatorial Atlantic (Gregg and Casey, 2004; Perez et al., 2005). Nevertheless, the model reproduces the major features of the observed surface chlorophyll fields, including the spatial pattern and magnitude for the equatorial Atlantic.

3.2. Comparison of the spatial variability

We analyze zonal variations of physical and biogeochemical properties in the equatorial Atlantic Ocean. Fig. 7 displays shoaled mixed layer depth (MLD) and the ferricline (*i.e.*, iron = 75 nmol m^{-3}) from west to east. The model simulation shows that the averaged MLD and ferricline are ~40 m and ~80 m, respectively, which are in the observed ranges (see Fig. 6 in Bowie et al., 2002). There is a clear DBM below the mixed layer across the entire upwelling region, which differs from the equatorial Pacific that lacks a DBM in the upwelling region (see Fig. 2 in Wang et al., 2009b). The model also produces strong DCM below the mixed layer, which slightly shoals from ~90 m in the west to ~70 m in the east. The simulated chlorophyll ranges from ~0.2 mg C m^{-3} in the mixed layer to ~0.4 mg C m^{-3} at the DCM. While the surface chlorophyll is slightly higher in the equatorial Atlantic than in the Pacific, the subsurface chlorophyll is significantly higher with a deeper DCM in the former (see Maranon et al., 2000) than in the latter (see Le Borgne et al., 2002; Wang et al., 2009b). Interestingly, the averaged C:Chl ratio over the 5°N–5°S band shows similar vertical variations in both regions. For example, the averaged C:Chl ratio decreases from ~90 g:g near the surface to ~40 g:g at 100 m in the equatorial Pacific upwelling region, and from ~80 g:g to ~30 g:g in the equatorial Atlantic.

We also compare meridional variations of physical and biogeochemical properties for the upwelling regions of the equatorial Pacific and Atlantic. Fig. 8 reveals considerable differences in the MLD and the ferricline between the two regions. The MLD and ferricline are much shallower on the equator in the Pacific (~20 m and ~35 m, respectively) than in the Atlantic (~30 m and ~75 m, respectively). The equatorial Pacific shows little (weak) meridional asymmetry in MLD (ferricline) whereas the equatorial Atlantic exhibits pronounced asymmetrical features in both MLD and ferricline, *i.e.*, much deeper to the south than to the north, which is consistent with the observations (see Fig. 6 in Bowie et al., 2002).

Coincidently, there are large differences in the meridional–vertical distributions of phytoplankton biomass and chlorophyll between the two regions. For the equatorial Pacific Ocean, phytoplankton biomass is highest near the surface, with slightly higher values to the south than to the north. There is a modest DCM located between the mixed layer and ferricline. For the equatorial Atlantic, the model simulates strong DBM and DCM with considerably higher values to the north than to the south. In general, chlorophyll is significantly higher in the equatorial Atlantic than in the Pacific. Interestingly, phytoplankton biomass is similar in the mixed layer, but remarkably higher below the mixed layer in the Atlantic than in the Pacific. The model simulations show much weaker meridional and vertical variability in phytoplankton carbon to chlorophyll (C:Chl) ratio in the Atlantic than in the equatorial Pacific. While both regions reveal similar C:Chl ratios (~30 g:g) at 120 m, the equatorial Atlantic has much lower C:Chl

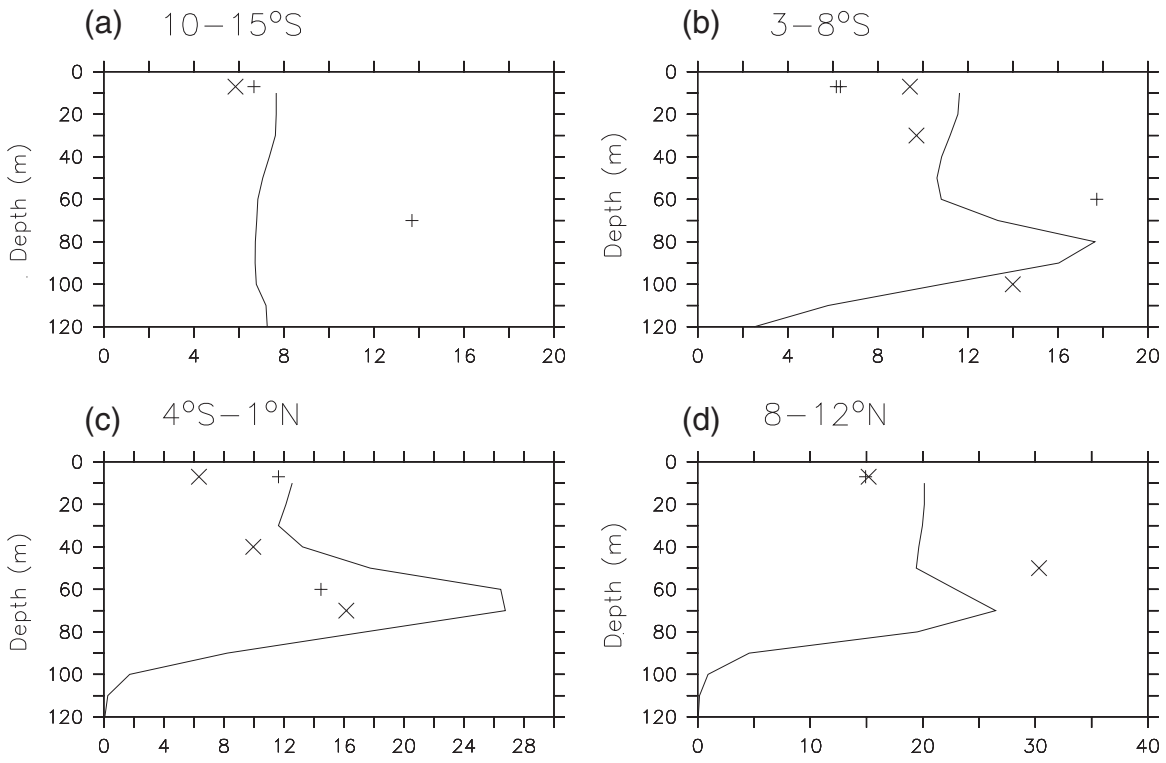

Fig. 5. Vertical distributions of phytoplankton carbon from model simulation (lines) and observation (symbols) during April–May, 1996 (Maranon et al., 2000) for (a) 10°S–15°S, (b) 3°S–8°S, (c) 4°N–1°S, and (d) 8°N–12°N.

ratios with a smaller range (~60–90 g:g) near the surface than the equatorial Pacific (~90–150 g:g).

3.3. Temporal variability

The model simulations display different temporal variability in the surface chlorophyll between the equatorial Pacific and the equatorial Atlantic for the period of 1990–2007 (Fig. 9). There is a clear front near the dateline in the equatorial Pacific, which reveals a remarkably large interannual variability that is associated with the El Niño/Southern Oscillation (ENSO) phenomenon (Le Borgne et al., 2002; Picaut et al., 2001; Wang et al., 2009b). West of the front, chlorophyll concentration is generally lower than 0.1 mg m^{-3} whereas east of the front, chlorophyll concentration has a range of 0.15–0.25 mg m^{-3}. In contrast, there is weak zonal variability and interannual variability, but a clear seasonality with a peak in boreal summer in the surface chlorophyll of the equatorial Atlantic, which have been observed in the equatorial Atlantic (Grodsky et al., 2008; Monger et al., 1997; Perez et al., 2005). Overall, the modeled surface chlorophyll concentration is higher in the equatorial Atlantic than in the equatorial Pacific upwelling region, which is consistent with satellite observation (see Fig. 1).

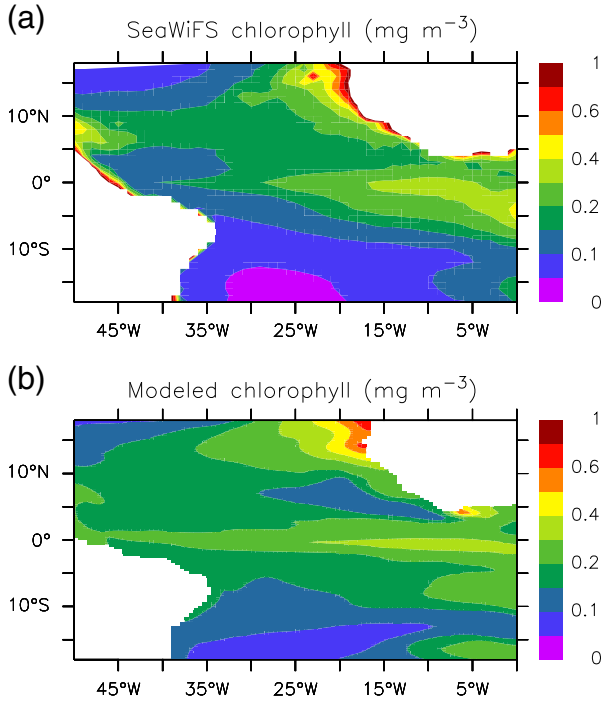

Fig. 6. Climatology (1997–2007) of surface chlorophyll from (a) SeaWiFS and (b) model simulation.

We further investigate how phytoplankton carbon, chlorophyll and C:Chl ratio vary interannually in the upwelling regions. In the equatorial Pacific (150°W–140°W, 5°N–5°S), phytoplankton carbon shows a gradual decrease with depth as one would expect from the significant influence of light attenuation in the euphotic zone (Fig. 10a). There are modest DCMs that vary from ~30 m in depth during non-El Niño years to ~90 m during the 1997/98 El Niño event (Fig. 10c). The model simulations show strong anomalies in the phytoplankton C:Chl ratio during the El Niño events when both phytoplankton and chlorophyll are decreased. However, there is a smaller decrease in phytoplankton carbon biomass than in chlorophyll during the warm ENSO periods (Fig. 11).

Fig. 10 also presents the time series of vertical distributions of phytoplankton biomass, chlorophyll and C:Chl ratio for the equatorial Atlantic. Unlike the equatorial Pacific upwelling region, phytoplankton biomass is generally low (~16 mg m^{-3}) in the upper euphotic zone, but highest (~24 mg m^{-3}) at ~70 m. Chlorophyll is generally higher in the euphotic zone with much stronger and deeper DCM in the equatorial Atlantic than in the equatorial Pacific. In addition, there is little interannual variability but clear seasonality that is associated

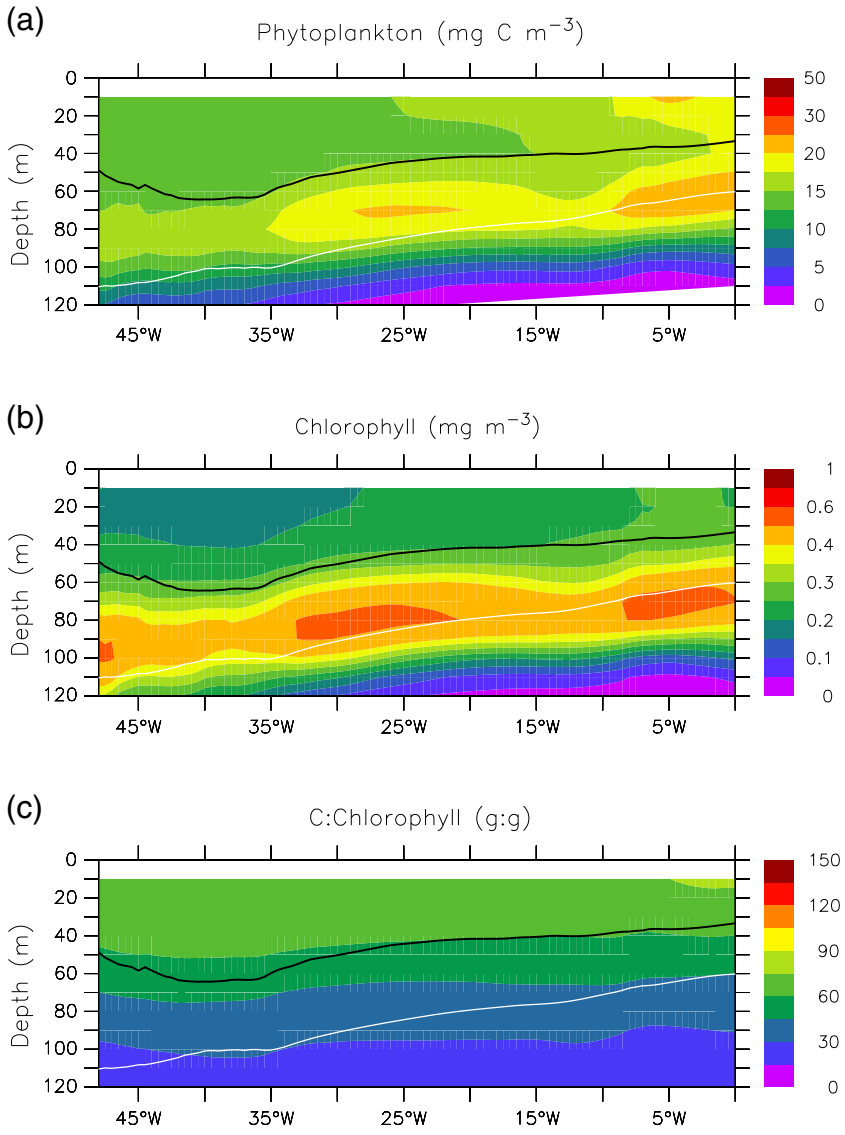

Fig. 7. Modeled zonal distributions of (a) phytoplankton, (b) chlorophyll, and (c) C:Chl ratio, averaged over 5°N–5°S for the period of 1990–2007 for the equatorial Atlantic. Superimposed black and white lines denote the depth for MLD and ferricline, respectively.

with the annual cycle of equatorial upwelling in the equatorial Atlantic (Weingartner and Weisberg, 1991). The model predicts weak temporal variability in the phytoplankton C:Chl ratio, except some degree of seasonality in the subsurface waters.

4. Discussion

Both the equatorial Pacific and Atlantic Oceans are referred to as upwelling regions with some degree of similarity in the surface chlorophyll. However, this modeling study demonstrates considerable differences in phytoplankton carbon and chlorophyll between the two basins in terms of magnitudes and variability. In this section, we discuss some of the main differences and underlying mechanisms, and explore uncertainties of our analyses and implications of our findings.

4.1. Chlorophyll and phytoplankton carbon

Despite of the similarity in the surface chlorophyll, the equatorial Atlantic shows a profound DCM (Maranon et al., 2000) that is similar to the widely observed DCM in the western warm pool of the equatorial Pacific (Le Borgne et al., 2002). Based on the SeaWiFS dataset, the surface chlorophyll averaged for the upwelling region is approximately 15% higher in the equatorial Atlantic than in the equatorial Pacific for the period of 1998–2007 (Table 2). However, the model simulations show that the basin-scale chlorophyll in the upwelling region of the equatorial Atlantic is significantly higher (>70%) for the upper 120 m relative to that in the equatorial Pacific.

While the modeled chlorophyll is the same as the SeaWiFS derived chlorophyll for the equatorial Atlantic, the model underestimates the variability of the surface chlorophyll (see Table 2). Apart from possible deficiency in the model forcing (*i.e.*, over-smoothed NCEP winds) and physical field in association with the standard cold-bias in most state of the art ocean models (see Murtugudde et al., 2002), the discrepancy may also reflect the difference in ecosystem structure between the simple model and a more complicated real ocean. For instance, the model does not include nitrogen fixation (*e.g.*, diazotrophs) that is an important process in the oligotrophic waters (LaRoche and Breitbarth, 2005; Mourino-Carballido et al., 2011). Nevertheless, the averaged C:Chl ratio from the model (74 g:g) is almost the same as the mean (75 g:g) for the surface water of the upwelling region (Maranon et al., 2000). Therefore, the model simulation provides realistic estimates of the mean fields for both chlorophyll and phytoplankton carbon for the equatorial Atlantic.

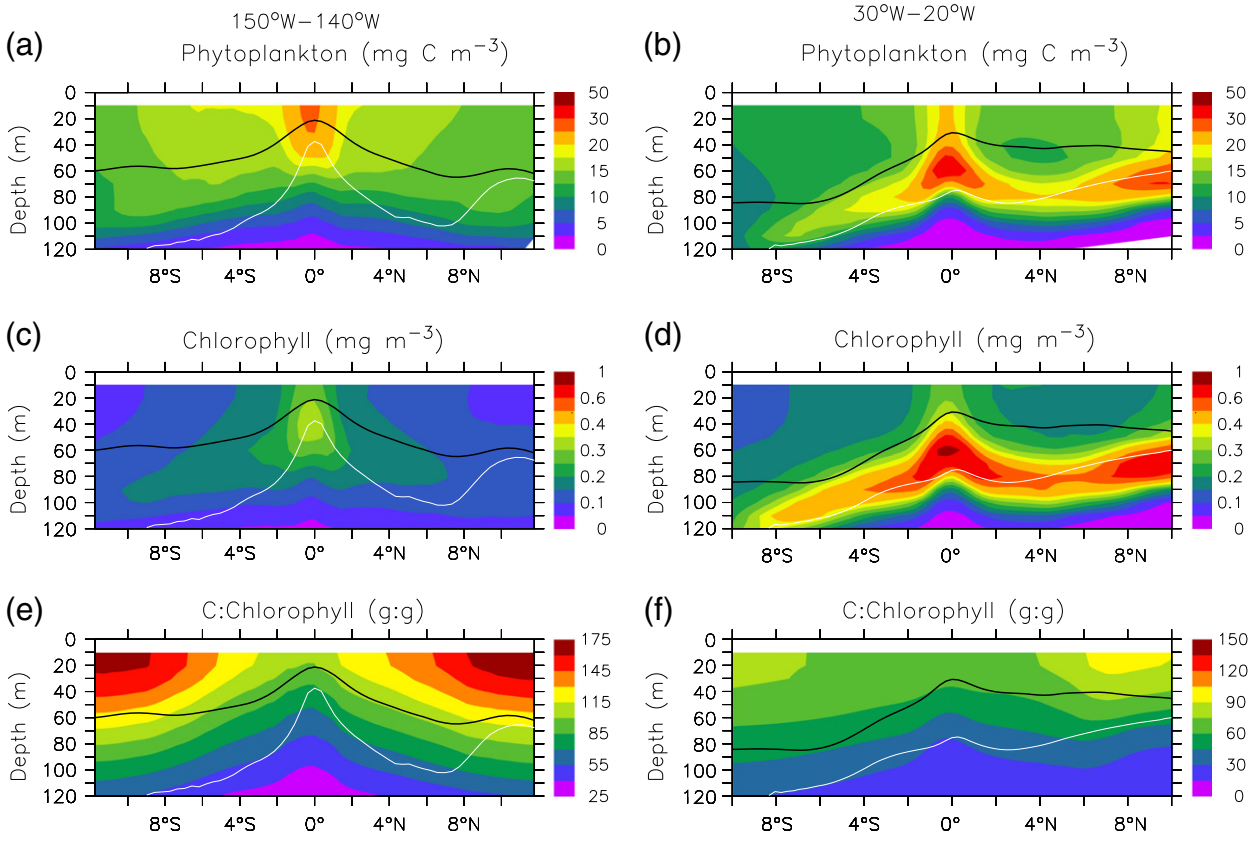

Fig. 8. Modeled climatology (1990–2007) of (a) and (b) phytoplankton, (c) and (d) chlorophyll, and (e) and (f) C:Chl ratio, in the equatorial Pacific (150°W–140°W, left column) and the equatorial Atlantic (30°W–20°W, right column), depth versus latitude. Superimposed black and white lines denote the depth for MLD and ferricline, respectively.

Assuming that the modeled phytoplankton biomass is overestimated by 10% (*i.e.*, the same as the modeled chlorophyll) for the equatorial Pacific, corrected averaged biomass would be ~19 mg C m^{-3} for the surface water and 1334 mg C m^{-2} for the upper 120 m. The latter is close to the observed average of 1370 mg C m^{-2} for the euphotic zone of the eastern equatorial Pacific (Taylor et al., 2011).

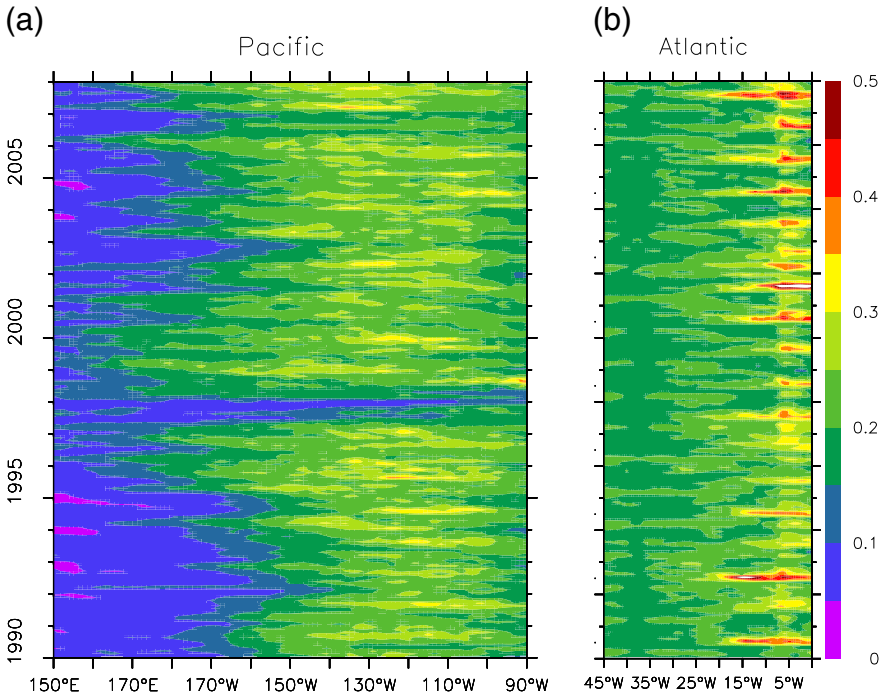

Fig. 9. Time-longitude contours of modeled surface chlorophyll (mg m^{-3}) in (a) the equatorial Pacific and (b) the equatorial Atlantic, averaged over 5°N–5°S for the period of 1990–2007.

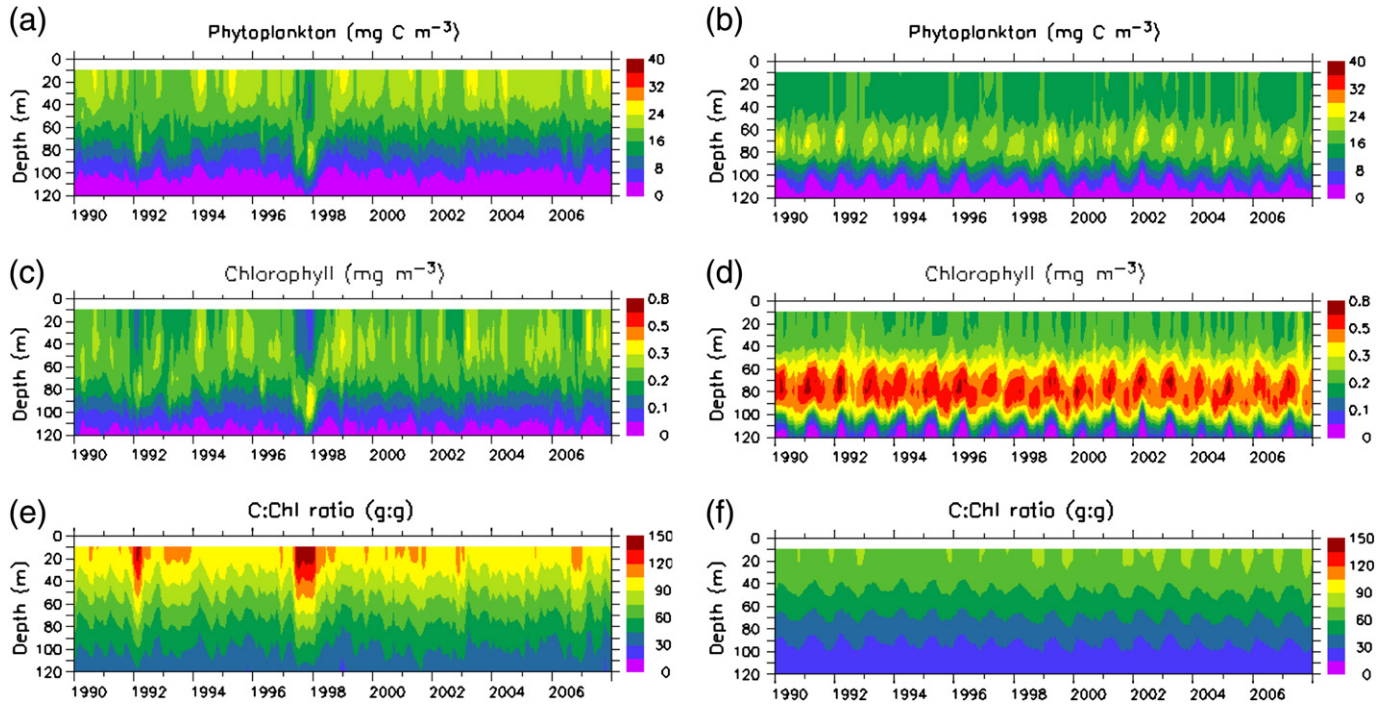

Fig. 10. Time-depth contours of (a) and (b) phytoplankton, (c) and (d) chlorophyll, and (e) and (f) C:Chl ratio in the equatorial Pacific (left column: averaged over the area of 150°W–140°W, 5°N–5°S), and in the equatorial Atlantic (right column: averaged over the area of 30°W–20°W, 5°N–5°S).

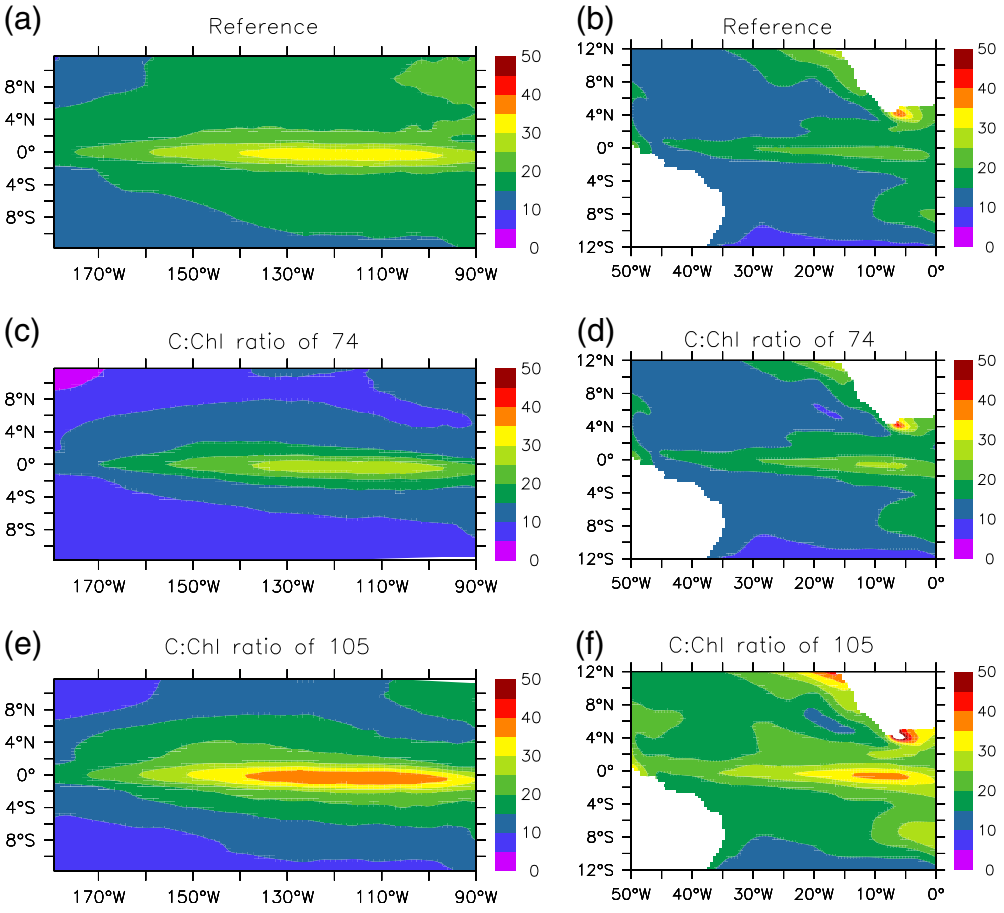

Fig. 11. Phytoplankton biomass (mg C m^{-3}) in surface water from (a) and (b) reference simulation with a variable C:Chl ratio, and generated from model chlorophyll using (c) and (d) a constant C:Chl ratio of 74 g:g, and (e) and (f) a constant C:Chl ratio of 105 g:g.

Table 2
Minimum (Min.), maximum (Max.), mean and standard deviation (S.D.) of the modeled chlorophyll and phytoplankton carbon biomass and observed surface chlorophyll from the SeaWiFS dataset for the period of 1997–2007.

Parameter	Depth	Unit	Pacific (180°W–90°W, 5°N–5°S)				Atlantic (45°W–0°W, 5°N–5°S)			
			Min.	Max.	Mean	S.D.	Min.	Max.	Mean	S.D.
SeaWiFS chlorophyll	Surface	mg m^{-3}	0.11	0.32	0.18	0.025	0.14	0.42	0.21	0.063
Model chlorophyll	Surface	mg m^{-3}	0.10	0.26	0.20	0.023	0.18	0.31	0.21	0.027
	0–120 m	mg m^{-2}	17.1	22.4	19.9	4.1	30.1	35.8	32.9	5.5
Model carbon	Surface	mg C m^{-3}	14.0	24.3	21.1	1.5	13.4	21.1	15.9	1.6
	0–120 m	mg C m^{-2}	1384	1651	1482	42.5	1480	1725	1565	39.6
Model C:Chl ratio	Surface	g:g	95	142	105	6.7	70	79	74	1.8
	0–120 m	g:g	61	96	74	5.2	46	54	50	1.8

Thus, for the surface water, the equatorial Pacific has ~20% higher phytoplankton biomass despite lower chlorophyll concentration; And for the entire euphotic zone, phytoplankton biomass is ~20% higher in the equatorial Atlantic than the equatorial Pacific. The difference in the surface phytoplankton carbon simply reflects the higher phytoplankton C:Chl ratios in the equatorial Pacific whereas the difference in the subsurface water is due to pronounced DBMs existing in the equatorial Atlantic.

4.2. Response of phytoplankton C:Chl ratio to environmental conditions

It is well known that phytoplankton C:Chl ratio decreases with depth owing to a phenomenon called "photoacclimation". However, less is known about the large scale spatial and temporal variations in phytoplankton C:Chl ratio although a wide range (from <30 g:g to >200 g:g) has been reported (*e.g.*, Le Bouteiller et al., 2003; Maranon, 2005; van Leeuwe and De Baar, 2000). While it is accepted that environmental conditions (*e.g.*, nutrients, light and temperature) regulate C:Chl ratio in phytoplankton cells, it is not well understood how these factors combine their influences. There have been controversial findings on the relationship between C:Chl ratio and size of phytoplankton cells. For instance, Le Bouteiller et al. (2003) reported higher C:Chl ratio in small cells than in large cells in the equatorial Pacific Ocean whereas Perez et al. (2006) found higher C:Chl ratio in larger cells (186 g:g) than in picoplankton (77 g:g) in the Atlantic subtropical gyres. A recent study (Taylor et al., 2011) reported lower C:Chl ratio (<70 g:g) during the Equatorial Biocomplexity (EB) cruises for the eastern equatorial Pacific, relative to previous studies (*e.g.*, Brown et al., 2003). The explanation for the difference may be spatial and/or temporal variation in association with biogeochemical fields. As discussed by Kaupp et al. (2011), iron concentration was considerably higher during the EB study than earlier studies.

While the response of C:Chl ratio to environmental conditions is complicated, the differences between the equatorial Pacific and Atlantic may be partly associated with nutrient conditions. The equatorial Pacific is strongly iron limited, without a nitracline in the upwelling region (Wang et al., 2009a), whereas the equatorial Atlantic experiences nitrogen limitation (Figure S2) with a profound nitracline below the mixed layer (Fig. 4). The stronger iron limitation in the Pacific as opposed to the Atlantic is well documented (*e.g.* Behrenfeld and Kolber 1999). The higher C:Chl ratios in the equatorial Pacific may result from a stronger iron limitation in the surface water (Landry et al., 2000), relative to the equatorial Atlantic. On the other hand, higher nitrate in the lower euphotic zone would lead to more biological activity, and thus higher biomass, in the subsurface water of the equatorial Atlantic.

4.3. Spatial and temporal variability

The equatorial oceans are characterized as strong upwelling that brings nutrient-rich deep water to the surface, which leads to relatively higher biological production. While both the equatorial Pacific and Atlantic Oceans experience seasonality in upwelling, the maximum is in boreal fall in the former (Wang et al., 2009b), but in boreal summer in the latter (Christian and Murtugudde, 2003). It appears that the seasonality in both physical (*e.g.*, SST and MLD) and biogeochemical (*e.g.*, ferricline) fields is much stronger in the Atlantic than in the Pacific upwelling region (Figures S3 and S4). For instance, the equatorial Atlantic reveals a clear seasonal pattern in the subsurface with higher phytoplankton biomass during the first half of the year, corresponding with the shoaling of both MLD and ferricline.

Our model simulations demonstrate that there is weak interannual variability in the timing and strengthening of the seasonal upwelling in the equatorial Atlantic, but profound interannual variability in the equatorial Pacific (Figs. 9 and 10). Particularly, the upwelling region in the equatorial Pacific shows strong anomalies during the warm phase of the ENSO (*i.e.*, in 1992 and 1997), showing an increased C:Chl ratio in the upper water column and a deepened DCM. These anomalies are a result of weakening of the trade winds during the El Niño periods, which reduces the equatorial upwelling thus nutrient concentrations in the euphotic zone (Wang et al., 2009b).

Apart from the difference in temporal variability, there is also a large difference in the asymmetric features, *i.e.*, much greater in the equatorial Atlantic than the equatorial Pacific. These different features result from the differences in the interaction between upwelling response to external forcing (*e.g.*, trade winds) and internal relaxation of the thermocline and nutricline. The upwelling is generally stronger to the south of the equator in the Pacific, but to the north in the Atlantic; and the west–east slope in the upwelling region is much flatter in the Pacific than in the Atlantic.

4.4. Sensitivity of estimated phytoplankton biomass to C:Chl ratios in the model

Regional and global biogeochemical models often use a constant C:Chl ratio to compute chlorophyll from simulated phytoplankton biomass (*e.g.*, Wetzel et al., 2006). Our previous sensitivity study for the equatorial Pacific showed that with a constant C:Chl ratio, the model generated chlorophyll field displayed a weak DCM in the warm pool, and an overestimate of surface chlorophyll concentrations, particularly to the west (Wang et al., 2009a). Thus, a model with a constant C:Chl ratio underestimated the spatial variability in chlorophyll, particularly the west–east contrast in the equatorial Pacific.

In this study, we carry out a similar sensitivity study, by comparing the phytoplankton biomass from the reference simulation (*i.e.*, with a variable C:Chl ratio) with those generated from the model chlorophyll using (1) a constant C:Chl ratio of 74 g:g, the averaged C:Chl ratio for the equatorial Atlantic, and (2) a constant C:Chl ratio of 105 g:g, the averaged C:Chl ratio for the equatorial Pacific (see Table 2). Fig. 11 reveals large differences in the distribution of phytoplankton biomass. Apparently, using a constant C:Chl ratio of 74 significantly underestimates surface phytoplankton biomass for the

equatorial Pacific while using a constant C:Chl ratio of 105 causes remarkable overestimation of surface phytoplankton biomass for the equatorial Atlantic.

Table 3 further illustrates how C:Chl ratio affects the estimates of phytoplankton biomass in different regions. As expected, phytoplankton biomass would be higher in the Atlantic than in the Pacific if a constant C:Chl ratio is applied, owing to the relatively higher chlorophyll in the former. Particularly for the euphotic zone, integrated phytoplankton biomass in the Atlantic would be 55–83% higher than the Pacific, due to relatively stronger DCM and high chlorophyll in the lower euphotic zone in the latter. In addition, applying a constant C:Chl ratio would produce much larger spatial and temporal variations in phytoplankton biomass in both the Pacific and Atlantic Oceans, relative to the reference simulation. These analyses demonstrate that using a constant C:Chl ratio to derive phytoplankton biomass from chlorophyll datasets will result in considerable bias and uncertainties at region to global scales.

5. Conclusion

We have carried out basin-scale comparative analyses of phytoplankton carbon biomass and chlorophyll in the upwelling regions between the equatorial Pacific and Atlantic. Our modeling study indicates that for the surface water, the equatorial Pacific has higher phytoplankton biomass despite lower chlorophyll concentration. But, for the entire euphotic zone, phytoplankton biomass is higher in the equatorial Atlantic than the equatorial Pacific. The different phytoplankton dynamics in the surface water simply reflects larger phytoplankton C:Chl ratios in the equatorial Pacific that experiences strong iron limitation. On the other hand, the difference in the subsurface water is due to pronounced DBM in the equatorial Atlantic, which is the result of relatively higher nitrate in the lower euphotic zone. This modeling study not only adds insights on the spatial and temporal variability in phytoplankton carbon biomass across basins, but also emphasizes the importance of using variable C:Chl ratios to estimate carbon biomass at regional to global scales.

Acknowledgments

This work is supported by grants from the National Aeronautics and Space Administration. We are grateful for the anonymous reviewers for the constructive comments. The authors wish to acknowledge use of the Ferret program for analysis and graphics in this paper. Ferret is a product of NOAA's Pacific Marine Environmental Laboratory (Information is available at http://ferret.pmel.noaa.gov/Ferret/).

Table 3
Mean and standard deviation (S.D.)[a] of phytoplankton biomass for different regions during 1990–2007.

Region		Reference		C:Chl ratio = 74		C:Chl ratio = 105	
		Mean	(S.D.)	Mean	(S.D.)	Mean	(S.D.)
Surface water (mg C m^{-3})							
Pacific (180°W–90°W)	5°N–5°S	20.6	(1.8)	15.0	(2.1)	21.3	(2.9)
	10°N–10°S	18.4	(1.3)	12.0	(1.3)	17.0	(1.9)
Atlantic (45°W–0°W)	5°N–5°S	15.8	(1.5)	15.9	(1.9)	22.6	(2.7)
	10°N–10°S	15.1	(1.3)	14.7	(1.4)	20.9	(2.0)
0–120 m (g C m^{-2})							
Pacific (180°W–90°W)	5°N–5°S	1.49	(1.42)	1.47	(2.31)	1.56	(3.31)
	10°N–10°S	1.46	(1.35)	1.27	(1.63)	1.32	(2.20)
Atlantic (45°W–0°W)	5°N–5°S	1.56	(1.21)	2.46	(2.89)	2.43	(3.24)
	10°N–10°S	1.54	(1.22)	2.33	(2.93)	2.28	(3.32)

[a] Standard deviation is calculated over time.

Appendix A. Supplementary data

Supplementary data to this article can be found online at doi:10.1016/j.jmarsys.2012.03.004.

References

Armstrong, R.A., 2006. Optimality-based modeling of nitrogen allocation and photoacclimation in photosynthesis. Deep-Sea Res. Part II 53, 513–531.
Behrenfeld, M.J., Falkowski, P.G., 1997. Photosynthetic rates derived from satellite-based chlorophyll concentration. Limnol. Oceanogr. 42, 1–20.
Behrenfeld, M.J., Kolber, Z.S., 1999. Widespread iron limitation of phytoplankton in the South Pacific Ocean. Science 283, 840–843.
Behrenfeld, M.J., Maranon, E., Siegel, D.A., Hooker, S.B., 2002. Photoacclimation and nutrient-based model of light-saturated photosynthesis for quantifying oceanic primary production. Mar. Ecol. Prog. Ser. 228, 103–117.
Behrenfeld, M.J., Boss, E., Siegel, D.A., Shea, D.M., 2005. Carbon-based ocean productivity and phytoplankton physiology from space. Global Biogeochem. Cycles 19, GB1006 doi:1010.1029/2004GB002299.
Bowie, A.R., Whitworth, D.J., Achterberg, E.P., Mantoura, R.F.C., Worsfold, P.J., 2002. Biogeochemistry of Fe and other trace elements (Al, Co, Ni) in the upper Atlantic Ocean. Deep-Sea Res. Part I-Oceanogr. Res. Pap. 49, 605–636.
Brown, S.L., Landry, M.R., Neveux, J., Dupouy, C., 2003. Microbial community abundance and biomass along a 180 degrees transect in the equatorial Pacific during an El Nino–Southern Oscillation cold phase. J. Geophys. Res. 108, 8139 doi:8110.1029/2001JC000817.
Busalacchi, A.J., Picaut, J., 1983. Seasonal variability from a model of the tropical Atlantic-ocean. J. Phys. Oceanogr. 13, 1564–1588.
Carr, M.-E., Friedrichs, M.A.M., Schmeltz, M., Noguchi Aita, M., Antoine, D., Arrigo, K.R., Asanuma, I., Aumont, O., Barber, R., Behrenfeld, M., 2006. A comparison of global estimates of marine primary production from ocean color. Deep-Sea Res. Part II 53, 741–770.
Chavez, F.P., Buck, K.R., Service, S.K., Newton, J., Barber, R.T., 1996. Phytoplankton variability in the central and eastern tropical Pacific. Deep-Sea Res. Part II 43, 835–870.
Chavez, F.P., Pennington, J.T., Castro, C.G., Ryan, J.P., Michisaki, R.P., Schlining, B., Walz, P., Buck, K.R., McFadyen, A., Collins, C.A., 2002. Biological and chemical consequences of the 1997–1998 El Nino in central California waters. Prog. Oceanogr. 54, 205–232.
Chen, D., Rothstein, L.M., Busalacchi, A.J., 1994. A hybrid vertical mixing scheme and its application to tropical ocean models. J. Phys. Oceanogr. 24, 2156–2179.
Christian, J.R., Murtugudde, R., 2003. Tropical Atlantic variability in a coupled physical–biogeochemical ocean model. Deep-Sea Res. Part II 50, 2947–2969.
Doney, S.C., Lima, I., Moore, J.K., Lindsay, K., Behrenfeld, M.J., Westberry, T.K., Mahowald, N., Glover, D.M., Takahashi, T., 2009. Skill metrics for confronting global upper ocean ecosystem-biogeochemistry models against field and remote sensing data. J. Mar. Syst. 76, 95–112.
Faure, V., Pinazo, C., Torreton, J.P., Douillet, P., 2006. Relevance of various formulations of phytoplankton chlorophyll a: carbon ratio in a 3D marine ecosystem model. CR Biol. 329, 813–822.
Feely, R.A., Boutin, J., Cosca, C.E., Dandonneau, Y., Etcheto, J., Inoue, H.Y., Ishii, M., Quéré, C.L., Mackey, D.J., McPhaden, M., Metzl, N., Poisson, A., Wanninkhof, R., 2002. Seasonal and interannual variability of CO_2 in the equatorial Pacific. Deep-Sea Res. Part II 49, 2443–2469.
Foltz, G.R., McPhaden, M.J., 2004. The 30–70 day oscillations in the tropical Atlantic. Geophys. Res. Lett. 31, L15205 15210.11029/12004GL020023.
Geider, R.J., La Roche, J., 2002. Redfield revisited: variability of C:N:P in marine microalgae and its biochemical basis. Eur. J. Phycol. 37, 1–17.
Geider, R.J., Macintyre, H.L., Kana, T.M., 1996. A dynamic model of photoadaptation in phytoplankton. Limnol. Oceanogr. 41, 1–15.
Geider, R.J., MacIntyre, H.L., Kana, T.M., 1997. Dynamic model of phytoplankton growth and acclimation: responses of the balanced growth rate and the chlorophyll a: carbon ratio to light, nutrient-limitation and temperature. Mar. Ecol. Prog. Ser. 148, 187–200.
Geider, R.J., Macintyre, H.L., Kana, T.M., 1998. A dynamic regulatory model of phytoplanktonic acclimation to light, nutrients, and temperature. Limnol. Oceanogr. 43, 679–694.
Gent, P.R., Cane, M.A., 1989. A reduced gravity, primitive equation model of the upper Equatorial Ocean. J. Comput. Phys. 81, 444–480.
Gregg, W.W., Casey, N.W., 2004. Global and regional evaluation of the SeaWiFS chlorophyll data set. Remote Sens. Environ. 93, 463–479.
Grodsky, S.A., Carton, J.A., McClain, C.R., 2008. Variability of upwelling and chlorophyll in the equatorial Atlantic. Geophys. Res. Lett. 35, L03610 doi:03610.01029/02007GL032466.
Huete-Ortega, M., Calvo-Diaz, A., Grana, R., Mourino-Carballido, B., Maranon, E., 2011. Effect of environmental forcing on the biomass, production and growth rate of size-fractionated phytoplankton in the central Atlantic Ocean. J. Mar. Syst. 88, 203–213.
Ishizaka, J., Harada, K., Ishikawa, K., Kiyosawa, H., Furusawa, H., Watanabe, Y., Ishida, H., Suzuki, K., Handa, N., Takahashi, M., 1997. Size and taxonomic plankton community structure and carbon flow at the equator, 175°E during 1990–1994. Deep-Sea Res. Part II 44, 1927–1949.
Jiang, C., Thompson, L., Kelly, K.A., 2008. Equatorial influence of QuikSCAT winds in an isopycnal ocean model compared to NCEP2 winds. Ocean Model. 24, 65–71.

Kalnay, E., Kanamitsu, M., Kistler, R., Collins, W., Deaven, D., Gandin, L., Iredell, M., Saha, S., White, G., Woollen, J., Zhu, Y., Chelliah, M., Ebisuzaki, W., Higgins, W., Janowiak, J., Mo, K.C., Ropelewski, C., Wang, J., Leetmaa, A., Reynolds, R., Jenne, R., Joseph, D., 1996. The NCEP/NCAR 40-year reanalysis project. Bull. Am. Meteorol. Soc. 77, 437–471.

Kaupp, L.J., Measures, C.I., Selph, K.E., Mackenzie, F.T., 2011. The distribution of dissolved Fe and Al in the upper waters of the Eastern Equatorial Pacific. Deep-Sea Res. Part II: Top. Stud. Oceanogr. 58, 296–310.

Landry, M.R., Constantinou, J., Latasa, M., Brown, S.L., Bidigare, R.R., Ondrusek, M.E., 2000. Biological response to iron fertilization in the eastern equatorial Pacific (IronEx II). III. Dynamics of phytoplankton growth and microzooplankton grazing. Mar. Ecol. Prog. Ser. 201, 57–72.

LaRoche, J., Breitbarth, E., 2005. Importance of the diazotrophs as a source of new nitrogen in the ocean. J. Sea Res. 53, 67–91.

Le Borgne, R., Barber, R.T., Delcroix, T., Inoue, H.Y., Mackey, D.J., Rodier, M., 2002. Pacific warm pool and divergence: temporal and zonal variations on the equator and their effects on the biological pump. Deep-Sea Res. Part II 49, 2471–2512.

Le Bouteiller, A., Leynaert, A., Landry, M.R., Le Borgne, R., Neveux, J., Rodier, M., Blanchot, J., Brown, S.L., 2003. Primary production, new production, and growth rate in the equatorial Pacific: changes from mesotrophic to oligotrophic regime. J. Geophys. Res. 108, 8141 doi:8110.1029/2001JC000914.

Lefevre, N., Taylor, A.H., Gilbert, F.J., Geider, R.J., 2003. Modeling carbon to nitrogen and carbon to chlorophyll a ratios in the ocean at low latitudes: evaluation of the role of physiological plasticity. Limnol. Oceanogr. 48, 1796–1807.

Maranon, E., 2005. Phytoplankton growth rates in the Atlantic subtropical gyres. Limnol. Oceanogr. 50, 299–310.

Maranon, E., Holligan, P.M., Varela, M., Mourino, B., Bale, A.J., 2000. Basin-scale variability of phytoplankton biomass, production and growth in the Atlantic Ocean. Deep-Sea Res. Part I 47, 825–857.

McClain, C.R., Feldman, G.C., Hooker, S.B., 2004. An overview of the SeaWiFS project and strategies for producing a climate research quality global ocean bio-optical time series. Deep-Sea Res. Part II 51, 5–42.

Monger, B., McClain, C., Murtugudde, R., 1997. Seasonal phytoplankton dynamics in the eastern tropical Atlantic. J. Geophys. Res. 102, 12389–12411.

Mourino-Carballido, B., Grana, R., Fernandez, A., Bode, A., Varela, M., Francisco Dominguez, J., Escanez, J., de Armas, D., Maranon, E., 2011. Importance of N(2) fixation vs. nitrate eddy diffusion along a latitudinal transect in the Atlantic Ocean. Limnol. Oceanogr. 56, 999–1007.

Murtugudde, R., Seager, R., Busalacchi, A., 1996. Simulation of the tropical oceans with an ocean GCM coupled to an atmospheric mixed-layer model. J. Climate 9, 1795–1815.

Murtugudde, R., Beauchamp, J., McClain, C.R., Lewis, M., Busalacchi, A.J., 2002. Effects of penetrative radiation on the upper tropical ocean circulation. J. Climate 15, 470–486.

Perez, V., Fernandez, E., Maranon, E., Serret, P., Garcia-Soto, C., 2005. Seasonal and interannual variability of chlorophyll a and primary production in the Equatorial Atlantic: *in situ* and remote sensing observations. J. Plankton Res. 27, 189–197.

Perez, V., Fernandez, E., Maranon, E., Moran, X.A.G., Zubkovc, M.V., 2006. Vertical distribution of phytoplankton biomass, production and growth in the Atlantic subtropical gyres. Deep-Sea Res. Part I 53, 1616–1634.

Picaut, J., Ioualalen, M., Delcroix, T., Masia, F., Murtugudde, R., Vialard, J., 2001. The oceanic zone of convergence on the eastern edge of the Pacific warm pool: a synthesis of results and implications for El Nino–Southern Oscillation and biogeochemical phenomena. J. Geophys. Res. 106, 2363–2386.

Raimbault, P., Slawyk, G., Boudjellal, B., Coatanoan, C., Conan, P., Coste, B., Garcia, N., Moutin, T., Pujo-Pay, M., 1999. Carbon and nitrogen uptake and export in the equatorial Pacific at 150 degrees W: evidence of an efficient regenerated production cycle. J. Geophys. Res. 104, 3341–3356.

Signorini, S.R., Murtugudde, R.G., McClain, C.R., Christian, J.R., Picaut, J., Busalacchi, A.J., 1999. Biological and physical signatures in the tropical and subtropical Atlantic. J. Geophys. Res-Oceans 104, 18367–18382.

Taylor, A.G., Landry, M.R., Selph, K.E., Yang, E.J., 2011. Biomass, size structure and depth distributions of the microbial community in the eastern equatorial Pacific. Deep-Sea Res. Part II: Top. Stud. Oceanogr. 58, 342–357.

van Leeuwe, M.A., De Baar, H.J.W., 2000. Photoacclimation by the Antarctic flagellate *Pyramimonas* sp (Prasinophyceae) in response to iron limitation. Eur. J. Phycol. 35, 295–303.

Wang, X.J., Christian, J.R., Murtugudde, R., Busalacchi, A.J., 2005. Ecosystem dynamics and export production in the central and eastern equatorial Pacific: a modeling study of impact of ENSO. Geophys. Res. Lett. 32, L02608 doi:02610.01029/02004GL021538.

Wang, X.J., Le Borgne, R., Murtugudde, R., Busalacchi, A.J., Behrenfeld, M., 2008. Spatial and temporal variations in dissolved and particulate organic nitrogen in the equatorial Pacific: biological and physical influences. Biogeosciences 5, 1705–1721.

Wang, X.J., Behrenfeld, M., Le Borgne, R., Murtugudde, R., Boss, E., 2009a. Regulation of phytoplankton carbon to chlorophyll ratio by light, nutrients and temperature in the Equatorial Pacific Ocean: a basin-scale model. Biogeosciences 6, 391–404.

Wang, X.J., Le Borgne, R., Murtugudde, R., Busalacchi, A.J., Behrenfeld, M., 2009b. Spatial and temporal variability of the phytoplankton carbon to chlorophyll ratio in the equatorial Pacific: a basin-scale modeling study. J. Geophys. Res.-Oceans 114, C07008. doi:10.1029/2008JC004942.

Weingartner, T.J., Weisberg, R.H., 1991. On the annual cycle of equatorial upwelling in the central Atlantic-Ocean. J. Phys. Oceanogr. 21, 68–82.

Westberry, T., Behrenfeld, M.J., Siegel, D.A., Boss, E., 2008. Carbon-based primary productivity modeling with vertically resolved photoacclimation. Global Biogeochem. Cycles 22, GB2024 2010.1029/2007GB003078.

Wetzel, P., Maier-Reimer, E., Botzet, M., Jungclaus, J., Keenlyside, N., Latif, M., 2006. Effects of ocean biology on the penetrative radiation in a coupled climate model. J. Climate 19, 3973–3987.